Multilevel Upscaling in Heterogeneous Porous Media *

J. David Moulton[1,2] Stephan Knapek[3] and Joel E. Dendy[2]

[1] Center for Nonlinear Studies and [2] Mathematical Modeling and Analysis
Los Alamos National Laboratory
Los Alamos, NM 87545

[3] Institut für Angewandte Mathematik
Abteilung für Wissenschaftliches Rechnen und Numerische Simulation
Universität Bonn, Wegelerstr. 6, D-53115, Bonn, Germany

January 1999

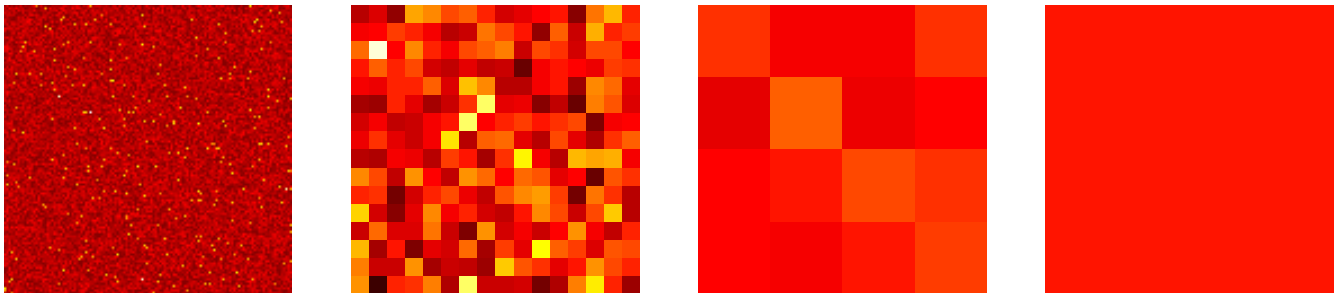

Abstract

The multiscale structure of heterogeneous porous media prevents a straightforward numerical treatment of the underlying mathematical flow models. In particular, fully resolved flow simulations are intractible and yet the fine-scale structure of a porous medium may significantly influence the coarse-scale properties of the solution (e.g., average flow rates). Consequently, homogenization or upscaling procedures are required to define approximate coarse-scale models suitable for efficient computation. Unfortunately, inherent in such a procedure is a compromise between its computational cost and the accuracy of the resulting coarse-scale solution. In general, most popular upscaling methods do not balance these competing demands. In this paper we highlight a new efficient, numerical method, which combines our recent work on multigrid homogenization (MGH) [23, 25] with the work of Dvořák [14] to compute bounded estimates of the homogenized permeability for single phase saturated flows. Our approach is motivated by the observation that the coarse-scale influence of multiscale structures are captured automatically by robust variationally defined multigrid methods. The effectiveness of this new algorithm is demonstrated with numerical examples.

*This research was performed under the auspices of the U.S. Department of Energy, under contract W-7405-ENG-36, and is to be referenced as LA-UR 99-4754.

1 Introduction:

The mathematical modeling of flow in porous media is playing an increasingly important role in the forecasting of petroleum reservoir performance, groundwater supply and subsurface contaminant flow. However, even with the increasing power of computers, a critical underlying problem in the numerical treatment of these models is the multiscale structure of heterogeneous geological formulations. Specifically, fully resolved simulations are computationally intractable because the length scales typically observed in sedimentary laminae range from the millimeter scale upward [27], while the simulation domain may be on the order of several kilometers. Yet, the fine-scale variations of the model's parameters (e.g., structure and orientation of laminae) significantly affect the coarse-scale properties of the solution (e.g., average flow rates). The complexity of this problem is further compounded by the increasing use of geostatistical techniques to compensate for the sparsity and uncertainty of field data through the generation of a large number of fine-scale realizations of a particular heterogeneous structure.

Fortunately, in many cases the physical measurements that can be made, or that are of interest, are not on the fine scale (e.g., pore scale) but are on an intermediate or even coarse scale (e.g., flow rate at a well). Hence, there is considerable interest in the development of upscaled or homogenized models in which the effective properties of the medium vary on a coarse scale suitable for efficient computation, but that accurately capture the influence of the fine-scale structure on the coarse-scale properties of the solution. Unfortunately, inherent in such a process is a compromise between its computational cost and the accuracy of the resulting solution. To demonstrate this competition, and the typical compromises that arise, we will consider the numerical treatment of the model for single-phase saturated flow that is given by [8],

$$\mathbf{u} = -\mathcal{K}(\mathbf{r})\nabla p\,, \tag{1}$$

$$\nabla \cdot \mathbf{u} = Q(\mathbf{r})\,, \tag{2}$$

where (1) defines the Darcy velocity $\mathbf{u}$ and (2) is a mass balance relation governing the pressure p and the source-sink term $Q(\mathbf{r})$. The permeability $\mathcal{K}(\mathbf{r})$ (which may be interpreted as the mobility, hydraulic conductivity, or diffusivity) is, in general, highly variable over a significant range of length scales.

In the following discussion we will work primarily with this model in its second order form,

$$-\nabla \cdot [\mathcal{K}(\mathbf{r})\nabla p] = Q(\mathbf{r}) \tag{3}$$

and, in particular, we will use the corresponding weak variational form

$$a(p,\phi) = \int_\Omega (\mathcal{K}(\mathbf{r})\nabla p, \nabla\phi) d\Omega = \int_\Omega Q\phi d\Omega \qquad \forall \phi \in H^1_{BC}(\Omega) \tag{4}$$

where $H^1_{BC}(\Omega) = \{\,\phi \in H^1(\Omega) |\, \phi \text{ subject to BCs}\}$, $a(p,\phi)$ is referred to as the energy inner product and $a(p,p)$ is the energy norm.

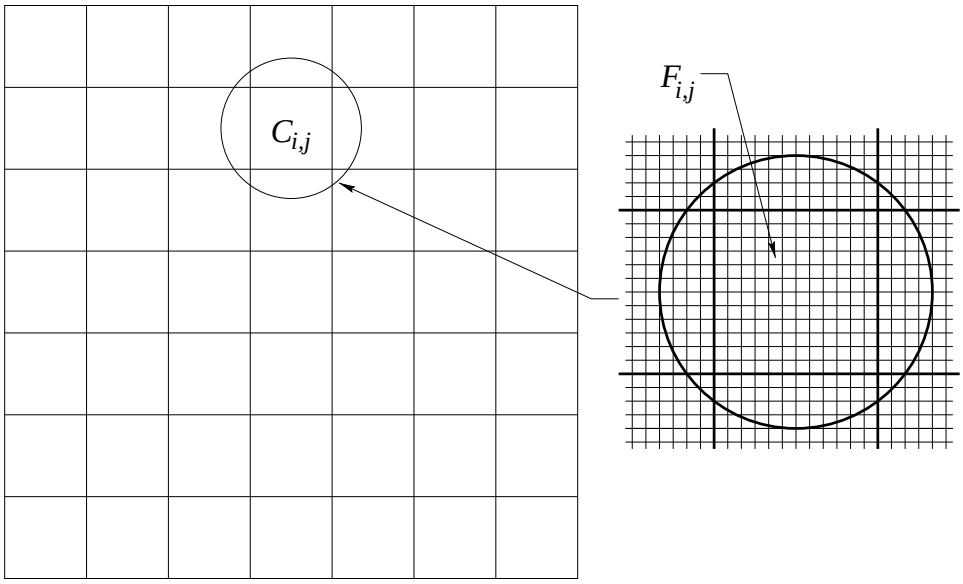

Figure 1: The permeability tensor of a porous medium is specified on each fine-scale cell $F_{i,j}$, and must be upscaled or homogenized over each coarse-scale or computational cell $C_{i,j}$.

This paper is organized as follows. In Section 2 a brief overview of homogenization and upscaling in porous media is given, with particular emphasis on single phase saturated flows. We also discuss the recent work of Dvořák which demonstrates that numerical methods naturally lead to upper and lower bounds of the homogenized permeability. In Section 3 we establish the connection between multilevel iterative solvers and discrete homogenized models. The resulting *multigrid homogenization* algorithm (MGH) is discussed in Section 4 and some numerical examples are present in Section 5. Finally we draw our conclusions and comment on future work.

2 Upscaling/Homogenization

The homogenization of the diffusion operator, and hence the permeability in (3), has been studied extensively during the last few decades (see [2, 17, 28]). An excellent introduction is provided by Holmes [16] and recently, two reviews of the literature related to single phase saturated flow were published [26, 30]. For the purposes of this paper it will necessarily suffice to highlight a few key points from this vast field.

We begin by making the common assumption that the fine-scale permeability tensor is constant over each fine-scale cell, $\mathcal{K}(\mathbf{r}) = \mathcal{K}_{i,j}$ for all $\mathbf{r} \in F_{i,j}$. The objective of a homogenization procedure for (3) is to define an equivalent coarse-scale permeability tensor that is constant over each coarse-scale cell, $\widehat{\mathcal{K}}(\mathbf{r}) = \widehat{\mathcal{K}}_{i,j}$ for all $\mathbf{r} \in C_{i,j}$, and which preserves certain coarse-scale properties of the fine-scale solution (see Figure 1).

The majority of existing homogenization methods involve local fine-scale computations and may be classified as either additive or Laplacian. Additive methods assume that the equivalent coarse-scale permeability may be defined as an explicit function of the fine-scale permeability. Motivated by their extremely low cost and the fact that there are isolated cases for which additive methods are exact (e.g., in one dimension $\widehat{\mathcal{K}}$ is given by the harmonic mean [2, 17]) these methods have been studied extensively (e.g., [11, 12, 13]). Unfortunately, it was concluded that, in general, there is no single rudimentary average that defines the exact effective permeability [30]. This inadequacy is a consequence of the interaction of different length scales. In particular a fine-scale isotropic permeability may give rise to a coarse-scale anisotropic flow. The simplest example of this behavior is an essentially one-dimensional structure in two dimensions, such as layered media. The equivalent permeability parallel to the layers may differ by orders of magnitude from the equivalent permeability perpendicular to the layers. Moreover, if the layers are not aligned with the coordinate axes (i.e., the principle axes of diffusion) a full tensor will be required to characterize the medium on the coarse-scale. Additive methods lack this critical property and hence, they may introduce extreme errors in coarse-scale simulations.

In contrast most Laplacian methods are capable of constructing full coarse-scale permeability tensors, even from an isotropic fine-scale permeability. These methods use the solution of local fine-scale problems (i.e., solve (3) over a coarse-scale cell $C_{i,j}$) to infer the coarse-scale permeability tensor $\widehat{\mathcal{K}}_{i,j}$ of the medium. Ideally, the boundary conditions for these local fine-scale problems would be consistent with the global fine-scale solution, but this solution is unknown. A number of schemes have been developed to work around this apparent short fall [26, 30] and have been applied with varying degrees of success. This may be surprising given the heuristic nature of these schemes; however, these methods may be viewed as approximations of more rigorous methods [20].

Specifically, homogenization theory for fine-scale periodic media (i.e., two well separated scales arise naturally) has a rigorous mathematical foundation (see, e.g., [2, 17]). Primarily born out of research in composite media the key results have been proven in a number of ways. In this summary we adopt the terminology of the two-scale asymptotic approach. Specifically, introducing a small parameter $\epsilon > 0$ to characterize the fine-scale we write $\rho = \mathbf{r}/\epsilon$ so that (3) may be expressed as a family of linear second order equations

$$\begin{aligned} L_\epsilon(p_\epsilon) &= -\nabla \cdot [\mathcal{K}(\rho)\nabla p_\epsilon] = Q(\mathbf{r}) \\ p_\epsilon &\quad \text{subject to suitable BCs} \end{aligned} \tag{5}$$

where L_ϵ is uniformly elliptic in ϵ. The pressure and the velocity converge weakly,

$$\begin{aligned} p_\epsilon &\rightharpoonup \widehat{p} && \text{weakly in } H^1_{BC}(\Omega) \\ \mathcal{K}(\rho)\nabla p_\epsilon &\rightharpoonup \widehat{\mathcal{K}}\,\nabla\widehat{p} && \text{weakly in } L_1(\Omega) \end{aligned}$$

where $\widehat{p}$ is the solution of the homogenized equation

$$\begin{aligned} \widehat{L}(\widehat{p}) &= -\nabla \cdot \left[\widehat{\mathcal{K}}\,\nabla\widehat{p}\right] = Q(\mathbf{r}) \\ \widehat{p} &\quad \text{subject to suitable BCs} \end{aligned}$$

The homogenized permeability may be expressed as,

$$\left(\widehat{\mathcal{K}}\,\xi,\xi\right) = \min_{\phi\in H_p^1(F)} a_\rho(\rho_\xi+\phi,\rho_\xi+\phi) \tag{6}$$

where ρ_ξ is a linear function such that $\xi = \nabla\rho_\xi$ is a constant vector in R^n, the periodic function space is $H_p^1(F) = \{\phi|\phi \in H^1(F), \phi \text{ periodic on } F\}$, and the local energy inner product is written

$$a_\rho(p,\phi) = \int_F (\mathcal{K}(\rho)\nabla_\rho p, \nabla_\rho\phi)\, dF\,. \tag{7}$$

Thus it is apparent that the homogenized permeability minimizes the energy. We note that the minimization implies that ϕ is the solution of

$$a_\rho(\rho_\xi+\phi,\psi) = 0\,, \qquad \forall\phi \in H_p^1(F) \tag{8}$$

Thus the significant cost of this approach is also highlighted: in n dimensions at least n fine-scale elliptic PDEs must be solved on each coarse-scale cell of the global domain. This cost is further compounded by the number of fine-scale realizations that may be required.

It is also important to note that these results have been extended to nearly periodic media (e.g., [6, 29]), thus accounting for the imperfections in real composite media. From our point of view the key difference is that the local problem (8) becomes a function of the coarse-scale variable, and similarly the homogenized permeability tensor. It is as an approximation to this result that the success of heuristic Laplacian methods are best understood. In this paper we will restrict our attention to the fine-scale periodic case, although the algorithm we propose does not require this assumption.

One method that attempts to bridge the gap between the low computational cost of additive methods and the superior accuracy of Laplacian methods is based on a numerical multilevel *renormalization* approach [18]. Specifically, renormalization uses the analogy of resistor networks to approximate an effective diagonal permeability tensor for a 2×2 block of fine-scale cells. Applying this technique recursively, a finite number of steps results in an equivalent diagonal permeability tensor for each coarse-scale cell $C_{i,j}$. Thus, the computational cost is comparable to additive methods, and moreover, the method automatically handles anisotropies that are aligned with the coordinate axes. However, there are two significant weaknesses. First, the resistor analogy implicitly defines artificial boundary conditions that impose one-dimensional flows in each of the coordinate directions. These artificial boundary conditions are applied at each step in the recursion, and therefore, may generate significant errors in the homogenized permeability [24]. Second, the homogenized permeability is at most a diagonal tensor, and hence, for cases in which the principle axes of diffusion are not aligned with the coordinate axes, the errors may be severe. In contrast our multigrid numerical homogenization algorithm [25] (also see, [22, 23]) captures the essential features of the rigorous asymptotic analysis (i.e., symmetric positive definite tensor) without requiring the solution of a single elliptic PDE.

2.1 Upper and Lower Bounds

Recently, Dvořák [14] noted that Ritz finite element (FE) discretizations of (8) could be used to compute an upper bound of the homogenized permeability. In particular, FE discretizations have test and trial functions that span a finite dimensional subspace of $H^1_p(F)$, and hence, they necessarily overestimate this minimal energy. He then noted that the dual formulation (i.e., the weak form of (1) and (2)) could be used to obtain a lower bound. In particular, in two dimensions he showed that the stream function formulation could be used to write this dual problem in the form,

$$\widehat{\mathcal{K}}^* = [\det(\widehat{\mathcal{K}}_{aux})]^{-1}\widehat{\mathcal{K}}_{aux} \tag{9}$$

where $\widehat{\mathcal{K}}_{aux}$ is given by the auxillary dual problem

$$(\widehat{\mathcal{K}}_{aux}\xi,\xi) = \min_{\phi\in H^1_p(F)} a^*_\rho(\rho_\xi+\nabla\phi,\rho_\xi+\nabla\phi) \tag{10}$$

in which a^*_ρ is given by (7) with $\mathcal{K}(\rho)$ replaced by $[\det(\mathcal{K}(\rho))]^{-1}\mathcal{K}(\rho)$. Hence, at least in two dimensions, it is straightforward to bound the homogenized permeability.

3 Multigrid Solvers

In many cases the numerical simulation of a mathematical model ultimately relies on the solution of a discrete, often linear, system of equations. Moreover, these systems are typically large and sparse, suggesting that the necessary efficiency would be best provided by iterative methods. An important class of iterative methods, namely multigrid methods, has received considerable attention since Brandt's [4] landmark paper in 1977. Early work on multigrid algorithms focused on the solution of second order elliptic PDEs, although subsequently these methods have been extended to a wide variety of applications (e.g., non-linear PDEs, integral equations). In particular, early research led to a multigrid algorithm with optimal efficiency (i.e., an unknown solution vector of length N is found in $O(N)$ operations) for the solution of finite difference discretizations of Poisson's equation. However, the application of this algorithm to diffusion equations with discontinuous coefficients (e.g., (3)) proved to be fragile, exhibiting convergence rates that were tightly coupled to the jumps or fine-scale structure of the diffusion coefficient. The solution of this problem proved challenging because it implicitly contains the same complexities as upscaling or homogenization procedures. To demonstrate this point and motivate our multigrid homogenization method, we first highlight the key components of a multigrid algorithm and then discuss the operator-induced variational coarsening that was first introduced in [1].

For readers unfamiliar with multigrid methods, an excellent introduction is given in [7], and reviews may be found in [5, 15]. A schematic of a multigrid V-cycle is shown in Figure 2

for which the key steps are:

- the residual on a particular grid is smoothed
  (i.e., it must be well approximated on a coarser grid)
- the residual is then *restricted* to the coarser grid
- repeat these steps recursively until the coarsest grid is reached
- solve on the coarsest grid
- *interpolate* to provide a correction on the next finer grid
- smooth the new residual
- repeat to undo the recursive coarsening

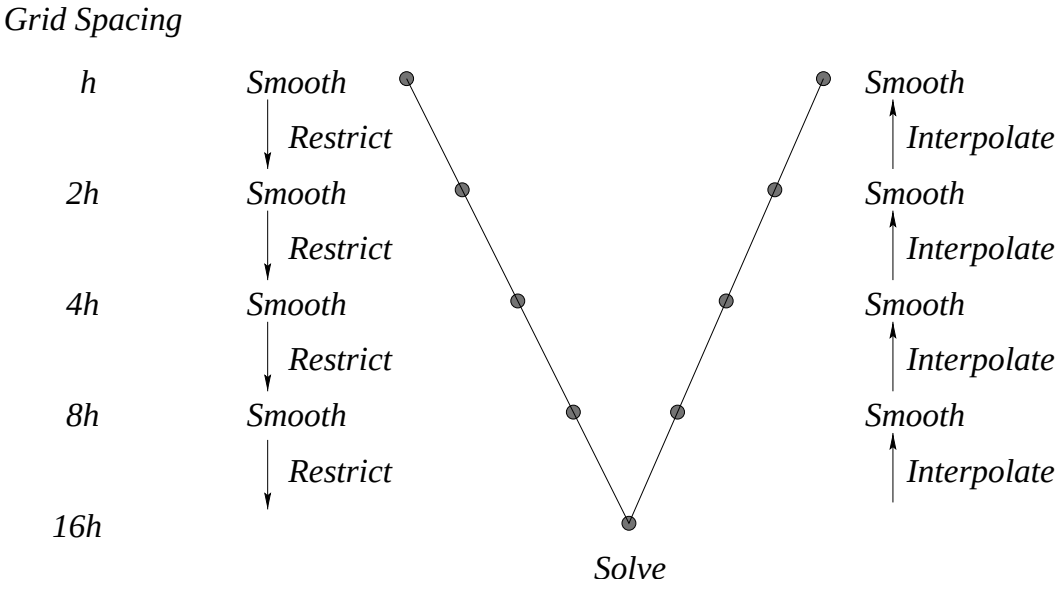

Figure 2: Schematic of the V-cycle multigrid iterative algorithm.

Thus, it is apparent that efficiency of a multigrid algorithm is tightly coupled to the effectiveness of the smoother (although this component is beyond the scope of this discussion), the coarse-grid operators

$$L_k \quad \text{– discrete operator on grid } k, \quad k = 1, 2, \ldots, (\textit{number of grids})-1$$

and the intergrid transfer operators,

$$\begin{aligned} I_{k-1}^{k} \quad & \text{– interpolation operator,} \quad \textit{grid } (k-1) \rightarrow \textit{grid } k \\ J_{k}^{k-1} \quad & \text{– restriction operator,} \quad \textit{grid } k \rightarrow \textit{grid } (k-1) \end{aligned}$$

Variational coarsening offers one means of defining L_{k-1} in terms of L_k, J_k^{k-1} and I_{k-1}^k. The development is given by Brandt [5] and follows naturally upon the restatement of the linear

system as an equivalent minimization problem. The resulting coarse-grid operator is

$$L_{k-1} = \left(J_{k-1}^k\right)^* L_k I_{k-1}^k \,, \tag{11}$$

and thus, to preserve symmetry we take $J_k^{k-1} = \left(I_{k-1}^k\right)^*$.

To highlight the connection between the variational definition of the coarse-grid opeators (11) and homogenization or upscaling procedures we consider the finite element discretization of (4). The fine-scale discrete operator (with $\{\psi_j^k\}_{j=1}^{n_k}$, $\{\varphi_j^k\}_{j=1}^{n_k}$ as trial and test functions on Level k) may be written

$$\left(L_k\right)_{ij} = \int_\Omega \left(\mathcal{K}(\mathbf{r})\nabla\psi_i^k, \nabla\varphi_j^k\right) d\Omega. \tag{12}$$

Denoting the elements of the restriction $J_k^{k-1} = (r_{ij})_{ij}$ and the elements of the interpolation $I_{k-1}^k = (p_{ij})_{ij}$ we have

$$\left(L_{k-1}\right)_{ij} = \left(J_k^{k-1} L_k I_{k-1}^k\right)_{ij} = \sum_{l,m} r_{jl} p_{mj} \left(L_k\right)_{lm} = \int_\Omega \left(\mathcal{K}(\mathbf{r})\nabla\Big\{\sum_m p_{mi}\psi_m^k\Big\}, \nabla\Big\{\sum_l r_{jl}\varphi_l^k\Big\}\right) d\Omega, \tag{13}$$

Therefore, if we define the new basis functions on level $k-1$ by

$$\varphi_j^{k-1} = \sum_l r_{jl}\varphi_l^k \text{ and } \psi_j^{k-1} = \sum_m p_{mj}\psi_m^k \tag{14}$$

we may write the discrete coarse-grid in the form

$$\left(L_{k-1}\right)_{ij} = \int_\Omega \left(\mathcal{K}(\mathbf{r})\nabla\psi_i^{k-1}, \nabla\varphi_j^{k-1}\right) d\Omega \tag{15}$$

Therefore prolongation and restriction are not only mappings between grid function spaces but may be viewed, via (14), as part of the discretization on coarse grids. It is in this way that the variational definition of the coarse-grid operator may be viewed as a discrete method for calculating homogenized or coarse-scale equations that capture the influence of the fine-scale heterogeneous structure.

However, variational coarsening is not complete without the definition of the interpolation operator. In fact, the choice of the interpolation operator is critical to the robustness and efficiency of the resulting multigrid algorithm. For example, from (15) it is apparent that the common choice of bilinear interpolation generates a coarse-scale model in which the homogenized permeability is given by the arithmetic average. Therefore, it is not surprising that use of bilinear interpolation leads to a fragile multigrid algorithm that is not suitable for practical applications in which the permeability (or components of the permeability tensor) exhibit fine-scale structure or vary discontinuously by orders of magnitude. A significantly better choice is operator-induced interpolation [1, 9] (also referred to as *matrix-dependent* interpolation) in which the entries in the fine-scale discrete operator are used to define an

interpolation that preserves certain known properties of the solution. In particular, in [25] it is shown that that Dendy's operator-induced interpolation [9] approximately enforces the continuity of the normal flux through the vertical face shown in Figure 3 in the weak integral sense

$$\lim_{x \to x^-} \int_{y_{j-1}}^{y_{j+1}} (\mathcal{F} \cdot \mathbf{x}) dy = \lim_{x \to x^+} \int_{y_{j-1}}^{y_{j+1}} (\mathcal{F} \cdot \mathbf{x}) dy \,. \tag{16}$$

The continuity of the normal flux is a fundamental property of the original PDE, one that bilinear interpolation violates. A discussion of the one-dimensional case, for which this approach is exact, is given in [15, 23].

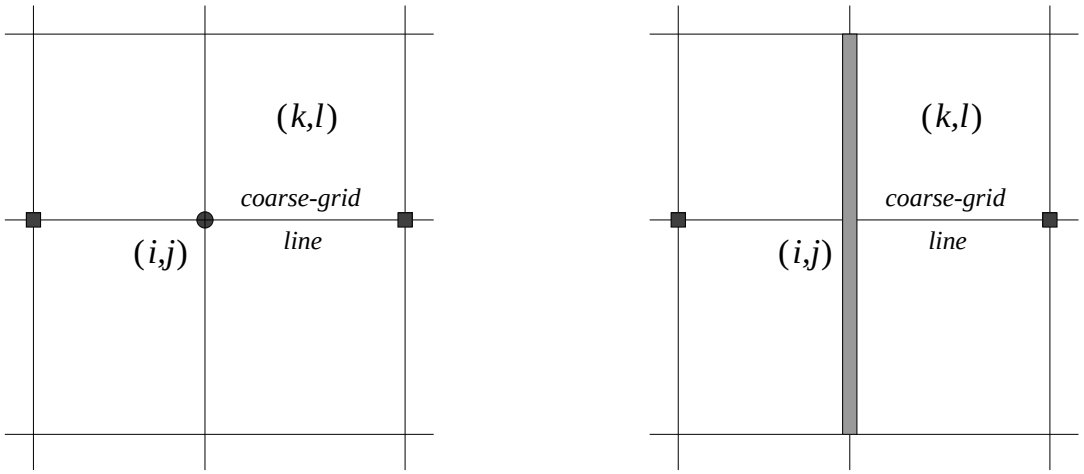

(a) (b)

Figure 3: (a) Interpolate the fine-grid point, "•", from the coarse-grid points, "blacksquares". (b) The objective is to preserve the continuity of the normal flux through the vertical interface at x_i (i.e., the shaded region).

4 Multigrid Homogenization

The objective of multigrid homogenization is to use operator-induced variational coarsening to compute a constant permeability tensor for each cell of the desired computational grid (i.e., a coarse-scale grid) without solving any local fine-scale flow problems. However, the operator-induced variational coarsening produces the coarse-grid discrete operator and not the permeability tensor. Thus, in [25] we developed a *local* expression for the cell-based permeability tensor in terms of the coarse-grid stencil (see Figure 4 for stencil nomenclature). For the fine-scale periodic case this result may be expressed in a simplified form.

Theorem 1 *Consider the conforming bilinear finite element discretization of (3) with constant permeability, $\mathcal{K}(x,y) = \widehat{\mathcal{K}}$ (i.e., the unknown homogenized coefficient) and subject to periodic boundary conditions on a rectangular domain Ω. In addition, assume a tensor-product grid with a constant grid spacing in each coordinate direction that is denoted by (hx, hy). An exact expression for the permeability tensor is given by*

$$\widehat{\mathcal{K}}_{k,l} = \begin{bmatrix} \frac{hx}{hy}\left\{S^{E}_{i,j} + S^{NE}_{i,j} + S^{NW}_{i+1,j}\right\} & \left(S^{NE}_{i,j} - S^{NW}_{i+1,j}\right) \\ \left(S^{NE}_{i,j} - S^{NW}_{i+1,j}\right) & \frac{hy}{hx}\left\{S^{N}_{i,j} + S^{NE}_{i,j} + S^{NW}_{i+1,j}\right\} \end{bmatrix}. \tag{17}$$

where (i,j) denotes the vertices and $(k,l) = (i+\frac{1}{2}, j+\frac{1}{2})$ denotes the cell centers of the grid.

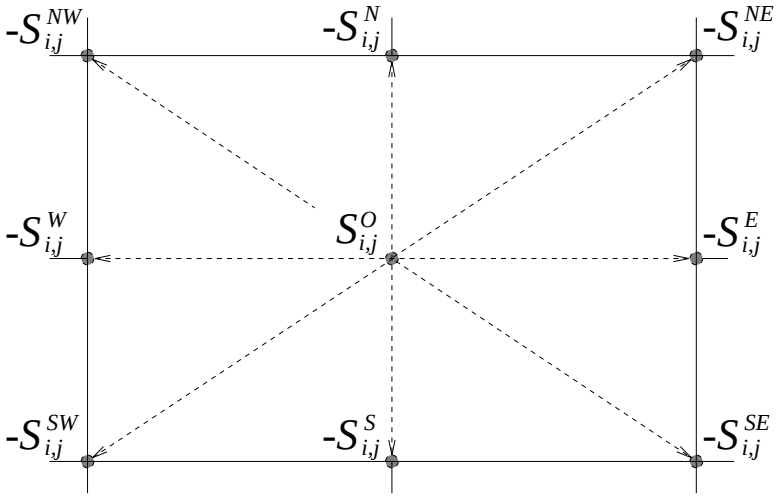

Figure 4: Compass-based definition of an arbitrary 9-point stencil.

The proof of Theorem 1 that is given in [25] utilizes a local flux analysis. Subsequently, in [21] we showed that this expresssion can be derived using the FE basis function approach that is given in [23]. To apply (17) it is necessary to ensure that the same stencil resides at each point in the coarsest grid. This may be accomplished by using a 3×3 tiling of the representative cell to define the homogenization domain Ω (see Figure 5). Thus, combining the expression for $\widehat{\mathcal{K}}$ given by (17), the analysis of Section 3 and the upper and lower bound results of Dvořák (Section 2.1) yields the numerical multigrid homogenization algorithm for periodic media (MGH).

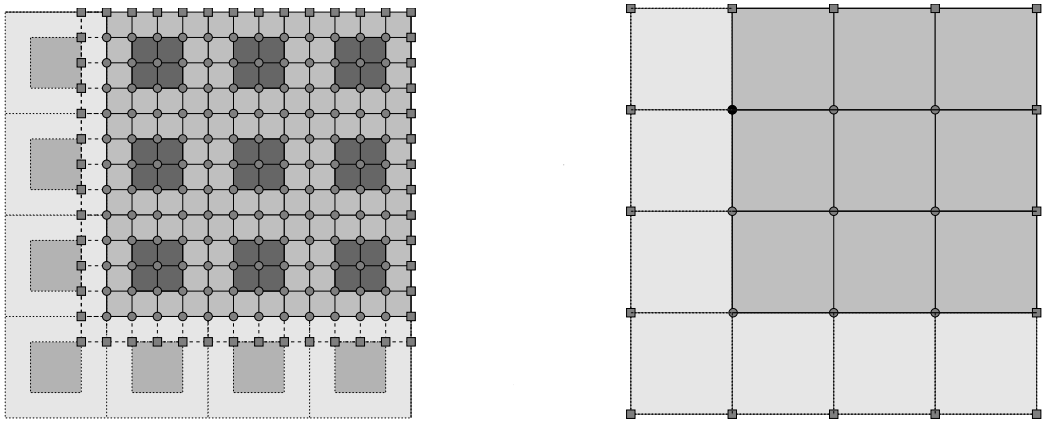

(a) (b)

Figure 5: (a) 12×12 computational mesh is superimposed on a 3×3 tiling of representative cells. (b) 3×3 computational mesh on the coarsest grid. The domain is now composed of homogenized cells.

ALGORITHM 1: *Multigrid Homogenization for Periodic Media (MGH)*

1. *Upper Bound*
   - For (8) construct the conforming bilinear FEM stencil for a 3×3 tiling of the representative cell on a sufficiently fine $3 \cdot 2^{k-1} \times 3 \cdot 2^{k-1}$ uniform grid.
   - Construct the coarse-grid operators with operator-induced coarsening [10].
   - Compute the upper bound $\widehat{\mathcal{K}}_u^{(bb)}$ on the 3×3 grid with (17).
2. *Lower Bound*
   - For the auxillary form of (8) construct the conforming bilinear FEM stencil for a 3×3 tiling of the representative cell on the previously selected grid.
   - Construct the coarse-grid operators with operator-induced coarsening [10].
   - Compute $\widehat{\mathcal{K}}_{aux}^{(bb)}$ on the 3×3 grid with (17).
   - Compute the lower bound $\widehat{\mathcal{K}}_l^{(bb)}$ with (9)
3. *Average the upper and lower bounds to obtain,* $\widehat{\mathcal{K}}_a^{(bb)}$

5 Examples:

5.1 Dependence on the Relative Diffusivity

In this example, we consider a square inhomogeneity (Figure 6) defined by,

$$\mathcal{K}(x,y) = \begin{cases} 1 \cdot I_2 & \forall (x,y) \in \Omega_0 \\ \lambda \cdot I_2 & \forall (x,y) \in \Omega_1 \end{cases}$$

to evaluate the dependence of the homogenized permeability tensor on the parameter λ. Symmetry guarantees that the homogenized permeability tensor is a scalar multiple of the identity. The upper and lower MGH bounds (obtained with a uniform 768×768 fine grid) are displayed in Figure 7. Also appearing in Figure 7 are the results of Bourgat [3] as well as the harmonic and arithmetic integral means. We note the excellent agreement of both the upper and lower MGH bounds with the asymptotic results over eight orders of magnitude in λ. The maximum error in these bounds is approximately 2%, and their arithmetic average (not shown) is virtually indistinguishable from the exact value on this scale.

We also observe that the arithmetic and harmonic bounds do not yield useful approximations of the homogenized permeability over the full range of λ. Specifically, the catastrophic failure of the harmonic mean as $\lambda \to 0^+$ is in contrast with an overestimation of approximately 10% in the arithmetic mean. Moreover, as $\lambda \to +\infty$, the harmonic mean yields approximately a 10% underestimation, while the arithmetic mean grows linearly, displaying an arbitrarily large error.

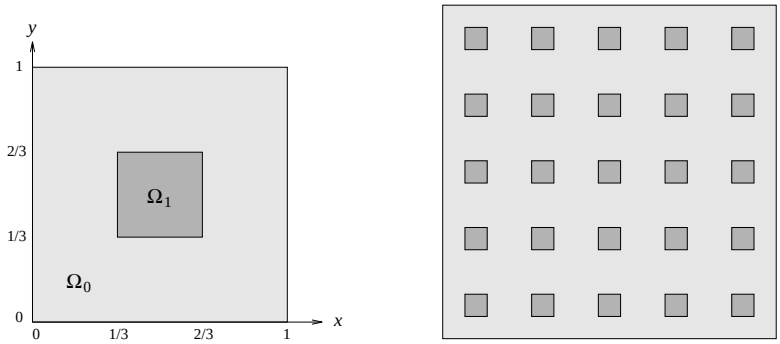

Figure 6: A representative cell with a square inhomogeneity of diffusivity λ and an area of 1/9 is shown beside the implied periodic structure.

5.2 Shape Dependence

The geometric dependence of the homogenized permeability tensor is demonstrated with three basic shapes: square, disk, and lozenge (i.e., rotated square), which are shown in

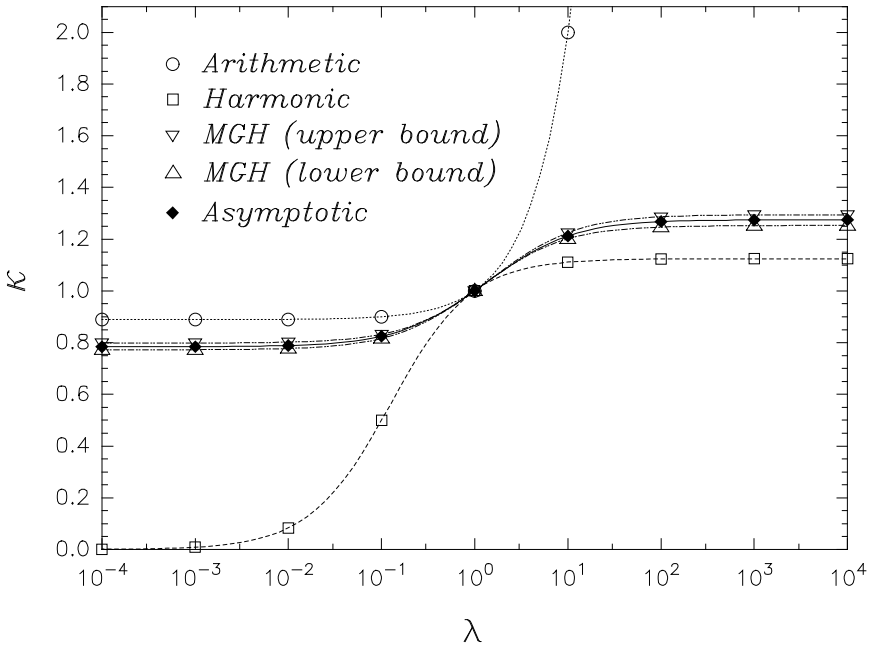

Figure 7: Dependence of homogenized diffusivities on the relative diffusivity λ.

Figure 8(a)-(c). The permeability tensor of these representative cells is defined by

$$\mathcal{K}(x,y) = \begin{cases} 1 \cdot I_2 & \forall (x,y) \in \Omega_0 \\ 10 \cdot I_2 & \forall (x,y) \in \Omega_1 \end{cases} .$$

In all cases, the area of Ω_1 is $1/4$. Moreover, symmetry ensures that the homogenized permeability tensor will also be a scalar multiple of the identity. A comparison of the results that we obtained with a 768×768 fine grid and those found in [3] is summarized in Table 1. These results demonstrate that the relative behavior of the upper and lower MGH bounds

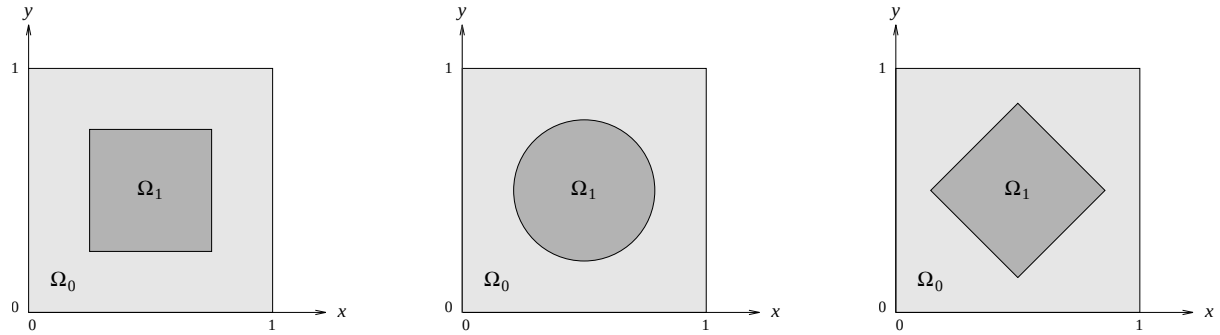

Figure 8: Three inhomogeneities with an area of $1/4$, but different shapes.

is similar to the rigorous treatment of Bourgat. Moreover the arithmetic average of these bounds yields an excellent approximation of the homogenized permeability, with relative errors of less than 1%. In contrast many popular alternatives are based solely on volume fraction (e.g., Hashin-Shtrikman bounds [26], simple integral averages) and hence, would yield the same result in all three cases. For example, the two-dimensional harmonic average is the same in all three cases and underestimates the asymptotic value by approximately 17%.

Table 1: Shape dependence of the homogenized permeability.

Shape	Bourgat	$\widehat{\mathcal{K}}_u^{(bb)}$	$\widehat{\mathcal{K}}_l^{(bb)}$	$\widehat{\mathcal{K}}_a^{(bb)}$	% Error
Square	1.548	1.5979	1.4923	1.545	0.19
Disk	1.516	1.5631	1.4740	1.519	0.20
Lozenge	1.573	1.6079	1.5114	1.560	0.83

5.3 A Dense Homogenized Permeability Tensor

To demonstrate that an isotropic inhomogeneity may lead to a dense tensor, Bourgat [3] considered the L–shaped region shown in Figure 9, with the following permeability tensor,

$$\mathcal{K}(x,y) = \begin{cases} 1 \cdot I_2 & \forall (x,y) \in \Omega_0 \\ 10 \cdot I_2 & \forall (x,y) \in \Omega_1 \end{cases} .$$

The asymptotic computation of Bourgat gives

$$\widehat{\mathcal{K}}^{(as)} = \begin{bmatrix} 1.915 & -0.101 \\ -0.101 & 1.915 \end{bmatrix} = Q \begin{bmatrix} 2.016 & 0 \\ 0 & 1.814 \end{bmatrix} Q^T ,$$

where the matrix of eigenvectors Q is given by

$$Q = \frac{1}{\sqrt{2}} \begin{bmatrix} -1 & 1 \\ 1 & 1 \end{bmatrix} .$$

Q defines the principal axes of diffusion, in this case a rotation of 45^o.

MGH also gives a full tensor and the average of the MGH upper and lower bounds, computed with a uniform 1536×1536 fine grid, is

$$\widehat{\mathcal{K}}^{(bb)} = \begin{bmatrix} 1.900 & -0.1385 \\ -0.1385 & 1.900 \end{bmatrix} = Q \begin{bmatrix} 2.039 & 0 \\ 0 & 1.762 \end{bmatrix} Q^T .$$

Remarkably, we obtain the exact principal axes of diffusion in this case. The only error is the scaling in each of these directions, approximately 1.1% and 2.9%, respectively. The error in the determinant is approximately 1.8%.

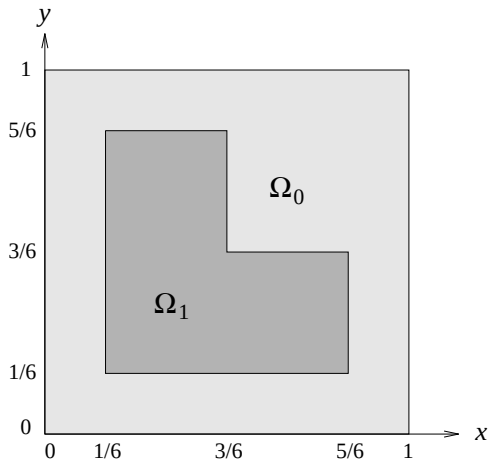

Figure 9: The homogenization of an L shaped inhomogeneity leads to a dense tensor.

5.4 Isotropic Random Permeability

Consider statistically isotropic porous media with the permeability defined by

$$\mathcal{K} = \kappa(x,y) \cdot I_2\,, \quad \kappa(x,y) = \zeta^{-\ln(\alpha)}\,, \quad \zeta \text{ uniformly distrubted in } (0,1)\,. \tag{18}$$

For this distribution it is possible to prove that the exact homogenized permeability is simply the geometric mean, $\widehat{\mathcal{K}} = \alpha \cdot I_2$ [19]. However, any finite realization of the random media

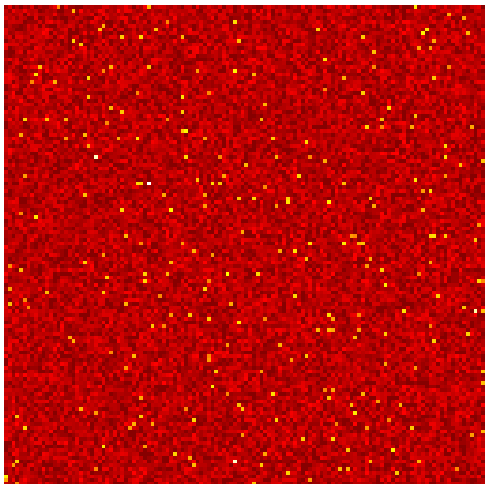

Figure 10: A 128×128 realization of the random permeability defined by (18).

will introduce a slight statistical anisotropy, and hence, the homogenized tensors that we compute with the MGH algorithm will also exhibit a slight anisotropy. For example, with

$\alpha = 10$, the arithmetic average of 10 samples (dimension 256×256) of the upper and lower MGH bounds gives

$$\widehat{\mathcal{K}}_a^{(bb)} = \begin{bmatrix} 8.2021 & -0.0016 \\ -0.0016 & 8.1632 \end{bmatrix}. \tag{19}$$

The slight anisotropy may be quantified by noting that the principle axes of diffusion have been rotated approximately 2.4^o and that the eigenvalues differ by approximately 0.5%. Thus, the approximation error associated with any of the homogenization methods is signifcantly larger than the statistical error, and so, to simplify the comparison we list the $(1,1)$ entries of the tensors in Table 2.

Once again the arithmetic and harmonic means exhibit severe errors. In fact, the error in all approximations of the homogenized permeability increases with increasing α. This is not surprising because the dynamic range of the fine-scale permability increases from approximately three orders of magnitude for $\alpha = 2$ to approximately thirteen orders of magnitude for $\alpha = 10$. Moreover, the standard deviation increases from approximately one order of magnitude for $\alpha = 2$ to approximately ten orders of magnitude for $\alpha = 10$. Nevertheless, the other methods, namely renormalization and MGH, provide reasonable approximations for this difficult problem. Specifically, for a $\alpha = 10$ renormalization understimates the homogenized permeability by $\approx 41\%$. Unfortunately, the MGH lower bound provides an estimate that is very similar to renormalization, displaying an error of 50% for $\alpha = 10$. This is significantly worse than the MGH upper bound, which for $\alpha = 10$ gives an error of only 10%. This mismatch in the magnitude of the errors leads to an average value of 8.20, an error of 18%. Although, it is dissapointing that this error is worse than that of the upper bound alone, it is vital to acknowledge that the error is now bounded. Further research will be required to understand precisely why the lower and upper bounds behave so differently in this case, particularly when they were found to be perform similarly in the earlier examples.

Table 2: Homogenization of a random permeability with exact $\widehat{\mathcal{K}} = \alpha \cdot I_2$.

α	$\widehat{\mathcal{K}}^{(am)}$	$\widehat{\mathcal{K}}^{(hm)}$	$\widehat{\mathcal{K}}_l^{(re)}$	$\widehat{\mathcal{K}}_l^{(bb)}$	$\widehat{\mathcal{K}}_u^{(bb)}$	$\widehat{\mathcal{K}}_a^{(bb)}$
2	3.21	1.70	1.88	1.824	2.092	1.96
5	$6.0E3$	2.61	3.73	3.361	5.519	4.44
10	$3.1E7$	3.30	5.82	4.982	11.42	8.20

6 Conclusions:

The new Multigrid Homogenization algorithm (MGH) offers a balance between computational expense and solution accuracy that is not found in other upscaling methods. In particular, it captures fine-scale geometric information that is missed entirely by rudimentary averages without requiring the solution of a single elliptic PDE. These properties of MGH were demonstrated with different symmetric shapes, and for an isotropic fine-scale

structure, the "L", that leads to a full tensor. MGH also achieved impressive accuracy over eight orders of magnitude in the relative permeability of a square heterogeneity. Moreover, in these cases, the averaging of the upper and lower bounds significantly improves the accuracy of the homogenized permeability. The method also performs well for the case of a homogeneous random media, which is more characteristic of porous media realizations. However, in this case the lower bound is in greater error than the upper bound. Future work will include the application of MGH to more realistic realizations of porous media and the testing of the resulting coarse-scale model through a series of flow simulations.

References

[1] R. E. Alcouffe, A. Brandt, J. E. Dendy, Jr. and J. W. Painter, "The Multi-grid Method for the Diffusion Equation with Strongly Discontinuous Coefficients", SIAM J. of Sci. and Stat. Comput., **2**, pp. 430–454.

[2] A Bensoussan, J.-L. Lions and G. Papanicolaou, *Asymptotic Analysis For Periodic Structures*, Studies in Mathematics and its Applications Volume 5, New York, 1978.

[3] J. F. Bourgat, "Numerical Experiments of the Homogenization Method for Operators with Periodic Coefficients", in *Computing Methods in Applied Science and Engineering, I*, Eds. R. Glowinski and J.-L. Lions, Springer, Versailles, pp. 330–356, 1977.

[4] A. Brandt, Multi–level adaptive solutions to boundary–value problems, Math. Comp. **31**, pp. 333-390, 1977.

[5] A. Brandt, Multigrid Techniques: 1984 Guide with Applications to Fluid Dynamics, The Weizmann Institute of Applied Science, Rehovot, Israel, 1984

[6] M. Briane, "Homogenization of a Non-Periodic Material", J. Math. Pures. Appl., **73**, pp. 47–66.

[7] W. L. Briggs, *A Multigrid Tutorial*, SIAM Books, Philadelphia, 1987.

[8] G. Dagan, "Flow and Transport in Porous Formations", Springer–Verlag, 1989.

[9] J. E. Dendy, Jr., "Black Box Multigrid", J. Comput. Phys., **48**, pp. 366–386, 1982.

[10] J. E. Dendy, Jr., "Black Box Multigrid for Periodic and Singular Problems", Appl. Math. Comput., **25**, pp. 1–10, 1988.

[11] A. J. Desbarats, "Spatial averaging of Hydraulic Conductivity in 3-Dimensional Hetergenous Porous-Media", Math. Geol., **24**, pp. 249–267, 1992.

[12] A. J. Desbarats,"Spatial Averaging of Transmissivity in Heterogeneous Fields With Flow Toward a Well", Water Resour. Res., **28**, pp. 757–767.

[13] L. J. Durlofsky, "Representation of Grid Block Permeability in Coarse Scale Models of Randomly Heterogeneous Porous-Media", Water Resour. Res., **28**, pp. 1791–1800, 1992.

[14] J. Dvořák, "A Reliable Numerical Method for Computing Homogenized Coefficients", MAT-Report 31, Mathematical Institute, Danish Technical University, Lyngby, Denmark, 1994.

[15] W. Hackbusch, *Multi-Grid Methods and Applications*, Springer Series in Computational Mathematics, Vol. 4, Springer–Verlag, Berlin, 1985

[16] M. H. Holmes, *Introduction to Perturbation Methods*, Texts in Applied Mathematics, No. 20, Springer–Verlag, New York, 1995.

[17] V. V. Jikov and S. M. Kozlov and O. A. Oleinik, *Homogenization of Differential Operators and Integral Functionals*, translated from Russian, Springer–Verlag, 1994.

[18] P. R. King, "The Use of Renormalization for Calculating Effective Permeability", Transport in Porous Media, **4**, pp. 37–58, 1989.

[19] S. M. Kozlov, "Averaging of Random Operators", Math. USSR Sbornik, pp. 167–180, **37**, 1980.

[20] S. Knapek and J. David Moulton, "A Unification of Multilevel Upscaling and Homogenization Methods for Porous Media", *in prep.*

[21] J.D. Moulton, S. Knapek, "A note on the Equivalence of Two Multigrid Homogenization Methods", *in prep.*

[22] S. Knapek, "Upscaling Techniques based on Subspace Correction and Coarse-Grid Approximations", In Situ, **22**, pp. 35-58, 1998.

[23] S. Knapek, "Matrix–Dependent Multigrid–Homogenization for Diffusion Problems", SIAM J. Sci. Comput., **20**, pp. 515–533, 1999.

[24] K. M. Malick, *Boundary effects in the successive upscaling of absolute permeability*, Masters Thesis, Stanford University, 1995.

[25] J. D. Moulton, J. E. Dendy and J. M. Hyman, "The Black Box Multigrid Numerical Homogenization Algorithm", J. Comput. Phys., **141**, pp. 1–29, 1998.

[26] Ph. Renard and G. de Marsily, "Calculating equivalent permeability: a review", Advances in Water Resources, **20**, pp. 253–278, 1997.

[27] G. E. Pickup, P. S. Ringrose, J. L. Jensen, and K. S. Sorbie, "Permeability Tensors for Sedimentary Structures", Mathematical Geology, **26**, pp. 227–250, 1994.

[28] E. Sanchez-Palencia, *Non–Homogeneous Media and Vibration Theory*, Lecture Notes in Physics, No. 127, Springer–Verlag, Berlin, 1980.

[29] S. Shkoller, "An approximate Homogenization Scheme for Nonperiodic Materials", Computers Math. Applic., **33**, pp. 15–34, 1997.

[30] X.-H. Wen and J. J. Gómez-Hernández, "Upscaling Hydraulic Conductivities in Heterogeneous Media: An Overview, Journal of Hydrology, **183**, pp. ix–xxii, 1996.